Supporting Information for "Characteristics of Station-Derived Convective Cold Pools Over Equatorial Africa"

Jannik Hoeller[1,2], Jan O. Haerter[1,2,3,4], Nicolas Da Silva[1]

[1]Integrated Modeling, Leibniz Centre for Tropical Marine Research, Fahrenheitstr. 6, 28359 Bremen, Germany

[2]Niels Bohr Institute, Copenhagen University, Blegdamsvej 17, 2100 Copenhagen, Denmark

[3]Physics and Earth Sciences, Constructor University Bremen, Campus Ring 1, 28759 Bremen, Germany

[4]Department of Physics and Astronomy, University of Potsdam, Karl-Liebknecht-Straße 32, 14476 Potsdam, Germany

Contents of this file

1. Text S1

2. Tables S1 to S2

3. Figures S1 to S2

Introduction

Text S1 describes the computation employed for mixing ratio, saturated mixing ratio, equivalent potential temperature, and temperature at the lifting condensation level. Table S1 presents geographic information regarding the deployed automatic weather stations. Table S2 summarizes statistics on the 4289 cold pools (CPs) which we identified

―――――

November 14, 2023, 8:04am

in five-minute near-surface data of twelve automatic weather stations in tropical Africa, recorded between January 1, 2019 and September 30, 2023. Fig. S1 shows the station-derived seasonal and diurnal cycle of near-surface equivalent potential temperature for different regions across equatorial Africa. Fig. S2 shows two probability distributions of satellite-derived properties of the identified cold pool gust fronts.

As in the main article, the statistics in Table S2, as well as the data in Fig. S1 and Fig. S2, are grouped based on the stations' deployment countries to enable an investigation of regional differences. In addition to general information on CP occurrence, Table S2 contains data on the strength of station-observed near-surface CP anomalies, as well as satellite-observed brightness temperatures. We assess the overall strength of a an anomaly by its largest extreme value in the time window from $t_0 - 20 \, min$ to $t_0 + 120 \, min$. Only for temperature, T, based on which the CP onset was defined, we consider the time window from t_0 to $t_0 + 120 \, min$ instead. For simplicity we refer to extreme values of anomalies as perturbations and denote them with a "δ". Whether the identified extreme values are maxima or minima depends on the variable and the detected CP: While we exclusively search for minima for T and equivalent potential temperature (θ_e), we look for maxima for wind gust speed (u_g), relative humidity (RH) and atmospheric pressure (p). For specific humidity, q, which may exhibit positive as well as negative perturbations, we search for both minima and maxima and consider the extreme value with the larger absolute value as perturbation. We define a maximum or minimum, respectively, as the largest local maximum or minimum in the corresponding time window. An instantaneous measurement $y(t)$ at time t is a local maximum if $y(t - 5 \, min) \leq y(t) > y(t + 5 \, min)$

November 14, 2023, 8:04am

and analogously for a local minimum. If a certain anomaly record of an identified CP has missing values or does not have an extreme value, we do not assign a perturbation. With respect to satellite-observed brightness temperatures, we evaluate the minimum brightness temperature, $BT_{10.8}^{min}$ by determining the minimum $10.8\,\mu m$ brightness temperature in the time window from $\hat{t}_0 - 60\,min$ to $\hat{t}_0 + 120\,min$, i.e., the corresponding time window around the satellite-observed CP onset, $\hat{t}_0$, which we define in the main article.

Text S1.

Based on the station-measured variables, we compute the saturated vapor pressure of water, e_{sat}, using equation 10 of Bolton (1980). We then derive the saturated mixing ratio, r_{sat}, by plugging e_{sat} and the station-measured atmospheric pressure, p, into the following equation from chapter 3.5.1 of Wallace and Hobbs (2006):

$$r_{sat} = 0.622 \frac{e_{sat}}{p - e_{sat}}. \tag{1}$$

To compute the mixing ratio, r, we adapt equation 3.64 of Wallace and Hobbs (2006). For the computation of the temperature at the lifting condensation level, T_{LCL}, and the equivalent potential temperature, θ_E, we employ equation 22 and 43, respectively, of Bolton (1980).

References

Bolton, D. (1980). The computation of equivalent potential temperature. *Monthly weather review*, *108*(7), 1046–1053.

Wallace, J. M., & Hobbs, P. V. (2006). *Atmospheric science: an introductory survey* (Vol. 92). Elsevier.

Table S1. Geographic information regarding the deployed automatic weather stations.

Station code	Country	Latitude [°N]	Longitude [°E]	Elevation [m]
TA00220	Uganda	1.21	32.74	1047
TA00222	Uganda	1.19	32.02	1069
TA00224	Uganda	0.57	32.64	1168
TA00410	DR Congo	0.82	24.46	464
TA00459	Nigeria	9.07	6.57	198
TA00580	Nigeria	7.84	9.78	162
TA00581	Nigeria	9.35	12.50	220
TA00584	Nigeria	7.80	8.62	104
TA00673	DR Congo	0.07	18.31	311
TA00717	Cameroon	3.90	11.89	734
TA00728	Cameroon	2.82	11.13	581
TA00730	Cameroon	3.47	11.49	665

Table S2. Summary of observed cold pool (CP) statistics including the total number of CPs and CPs per day, along with median values of different CP properties; sub- and superscripts indicate the interquartile range.

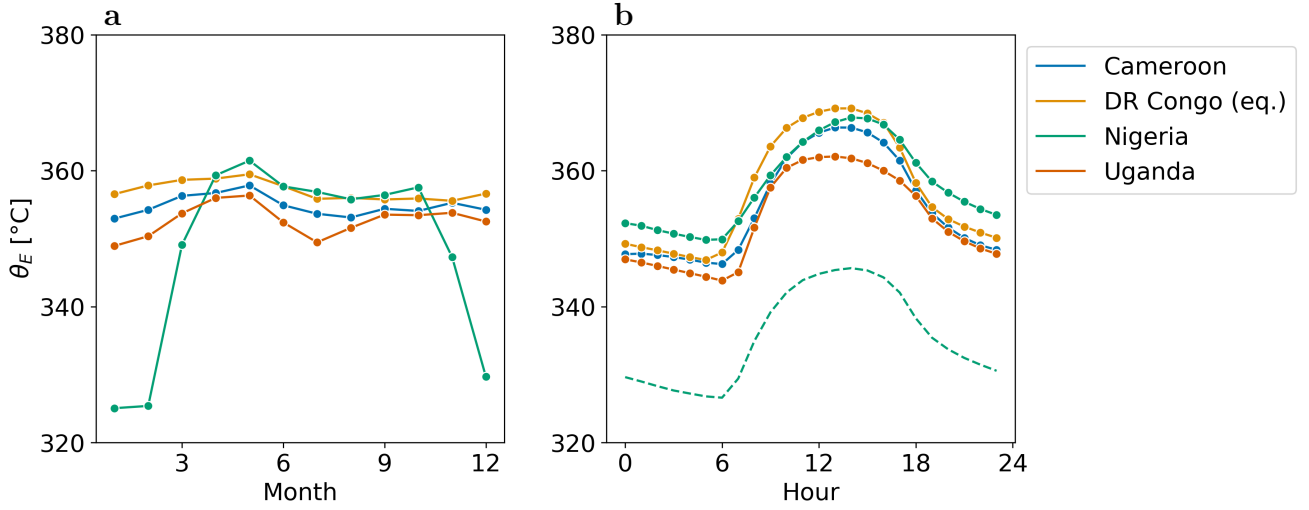|	Cameroon	DR Congo (eq.)	Nigeria	Uganda	All
$\#CPs$	791	652	1086	1760	4289
$\#CPs/day$	0.26	0.26	0.19	0.41	0.24
δT	$-4.90^{+1.20}_{-1.70}$	$-5.50^{+1.60}_{-1.80}$	$-5.30^{+1.40}_{-2.00}$	$-5.30^{+1.50}_{-2.00}$	$-5.20^{+1.40}_{-2.00}$
δq	$-3.06^{+1.07}_{-1.14}$	$-3.70^{+1.03}_{-1.23}$	$-3.68^{+1.30}_{-1.13}$	$-1.91^{+1.3}_{-0.95}$	$-2.80^{+1.31}_{-1.27}$
δu_g	$2.84^{+1.28}_{-0.99}$	$2.83^{+1.43}_{-1.00}$	$4.25^{+1.91}_{-1.69}$	$3.18^{+1.25}_{-0.90}$	$3.18^{+1.39}_{-1.04}$
$\delta\theta_e$	$-15.92^{+4.30}_{-5.09}$	$-18.45^{+4.57}_{-6.43}$	$-17.94^{+5.25}_{-5.66}$	$-12.51^{+4.50}_{-4.60}$	$-15.37^{+4.98}_{-5.48}$
δRH	$0.15^{+0.07}_{-0.07}$	$0.16^{+0.07}_{-0.08}$	$0.13^{+0.08}_{-0.05}$	$0.21^{+0.08}_{-0.07}$	$0.17^{+0.07}_{-0.07}$
δp	$1.23^{+0.77}_{-0.67}$	$1.35^{+0.75}_{-0.77}$	$1.65^{+0.83}_{-0.73}$	$0.85^{+0.60}_{-0.45}$	$1.18^{+0.75}_{-0.63}$
$BT^{min}_{10.8}$	212^{+22}_{-11}	208^{+23}_{-11}	206^{+27}_{-10}	222^{+30}_{-15}	214^{+30}_{-12}

Figure S1. Station-derived seasonal and diurnal cycle of near-surface equivalent potential temperature, θ_E. **a**, Mean θ_E for each month. Lines interpolate linearly between markers to facilitate the interpretation; colors indicate different regions. **b**, Mean θ_E at different times of the day. Each marker represents the mean value for a given 3-hour time interval, starting with the interval [0,3) for the marker at 0 LT. Lines and colors analogous to (a). The two lines for Nigeria represent rainy months (Apr–Oct, solid line with markers) and dry months (Nov–Mar, dashed).
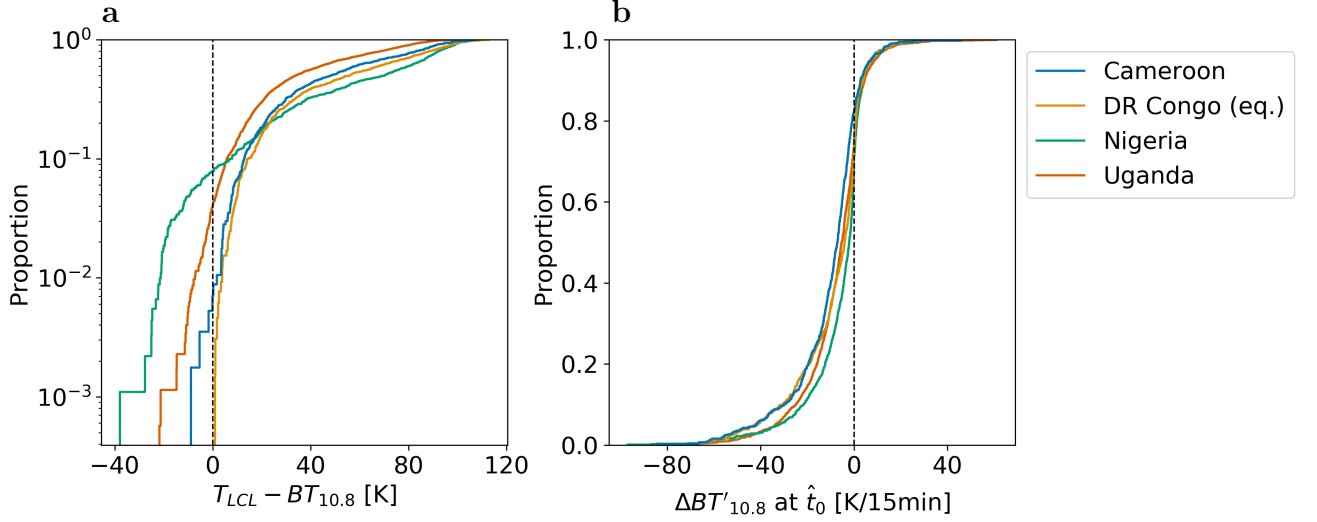
Figure S2. Probability distributions of satellite-derived cold pool (CP) properties. **a**, Distribution of the difference between the temperature at the lifting condensation level, T_LCL, and the corresponding $10.8\,\mu m$ brightness temperature, $BT_{10.8}$ of identified CP gust fronts; to increase the robustness, the difference is calculated based on the mean values of the two measurements at the nearest satellite time steps around the station-derived CP onset, t_0. Values below zero represent gust fronts with clear skies. Colors indicate different regions. **b**, Distribution of the temporal change of $10.8\,\mu m$ brightness temperature anomalies, $\Delta BT'_{10.8}$, at the satellite-observed CP onset, $\hat{t}_0$; colors analogous to (a).